

Influence of Axial Length on Thickness Measurements Using Spectral-Domain Optical Coherence Tomography

Tobias Röck,¹ Karl Ulrich Bartz-Schmidt,¹ Matthias Bramkamp,² Daniel Röck¹

¹Centre for Ophthalmology, University of Tübingen, Tübingen, Germany

²Department of General Medicine, Ruhr-University Bochum, Bochum, Germany

Correspondence: Tobias Röck, Centre for Ophthalmology, University of Tübingen, Schleichstraße 12, D-72076 Tübingen, Germany; Tobias.Roeck@med.uni-tuebingen.de.

Submitted: February 4, 2014

Accepted: September 29, 2014

Citation: Röck T, Bartz-Schmidt KU, Bramkamp M, Röck D. Influence of axial length on thickness measurements using spectral-domain optical coherence tomography. *Invest Ophthalmol Vis Sci.* 2014;55:7494-7498. DOI:10.1167/iov.14-14043

PURPOSE. The purpose of this study was to assess the influence of axial length on spectral-domain optical coherence tomography (SD-OCT) thickness measurements in patients with subretinal visual implants.

METHODS. Data from eight emmetropic pseudophakic eyes of eight patients with subretinal visual implants were analyzed retrospectively. These patients participated in the monocentric part of a multicenter trial. The axial length was measured in three short (<22.5 mm), three medium (22.51–25.50 mm), and two long (>25.52 mm) eyes. Using Heidelberg Spectralis, the known thickness of a subretinal implant microchip (70 μm) was measured on 15 images per eye with SD-OCT, using the software calipers.

RESULTS. The mean axial length was 20.8 \pm 0.8 mm in short eyes, 23.3 \pm 0.4 mm in medium eyes, and 26.3 \pm 0.5 mm in long eyes. We found in short eyes, in medium eyes, and in long eyes a mean value of microchip thickness measurements from SD-OCT of 82.9 \pm 1.4 μm , 70.5 \pm 1.3 μm , and 64.2 \pm 1.3 μm , respectively. The thickness measurements decreased in SD-OCT measurements with longer axial lengths significantly ($P < 0.0001$).

CONCLUSIONS. Axial length influences SD-OCT thickness measurements. Our findings demonstrate accuracy of the scaling in SD-OCT thickness measurements in emmetropic medium eyes. Caution is recommended when comparing the measured values of short and long eyes with the normative database of the instrument. There is a need for larger sample-size studies to confirm our results. (ClinicalTrials.gov number, NCT01024803.)

Keywords: spectral-domain optical coherence tomography (SD-OCT), in vivo measurement, axial length, subretinal visual implant, Heidelberg Spectralis

During the past two decades, there have been advances in optical coherence tomography (OCT) technology that have been used and improved on.^{1,2} Optical coherence tomography has become standard in the diagnosis and precise monitoring of patients with retinal and glaucomatous pathologies, for example, in assessing loss of retinal nerve fiber layer (RNFL) thickness³ or in the treatment of exudative age-related macular degeneration and diabetic macular edema.⁴ Quantitative retinal thickness measurements are of decisional value before subretinal implantation and the safety follow-up. Subretinal visual implants contain a light-sensitive microchip that replaces the function of degenerated photoreceptors in blind retinitis pigmentosa patients. The subretinal implant has been tested in human trials at the University of Tübingen since 2005.^{5–9} The subretinal implant consists of a 70- μm thin microchip with 1500 microphotodiodes and a sensor field area of 2800 $\mu\text{m} \times 2800 \mu\text{m}$. The microchip is implanted under the transparent retina into the macula region. Figure 1A shows red-free arterial-phase fluorescein angiography photography of a subretinal implant with a microchip on a polyamide film. Our results in 2014 found that axial length influences confocal scanning laser ophthalmoscopy (cSLO) and spectral-domain OCT (SD-OCT) size measurements.¹⁰ The investigation inspired us to examine the influence of axial length on thickness measurements using SD-OCT. To our knowledge, a depth measurement of the known thickness of subretinal implant

microchips (70 μm) in the living eye using SD-OCT had never been undertaken previously. Previous studies showed (using time-domain OCT and SD-OCT) that axial length influences optic nerve head and RNFL thickness measurements.^{11–16}

Our evaluation investigates the influence of axial length and the effect on thickness measurements in patients with subretinal visual implants using SD-OCT.

MATERIALS AND METHODS

Patients

We analyzed retrospectively data from eight patients who participated in the monocentric part of a multicenter trial. We selected for this evaluation eight pseudophakic emmetropic eyes (three males and five females, age range, 44 to 67, mean \pm standard deviation of 52.0 \pm 2.8 years) with retinitis pigmentosa (RP) and a subretinal visual implant.

All participants had a visual acuity of light perception before the implantation, detecting bright light without being able to localize the light source correctly. Further inclusion and exclusion criteria for the study have been published by Stingl et al.⁷ Written informed consent in accordance with the Declaration of Helsinki was obtained from all the subjects prior to inclusion in the study.

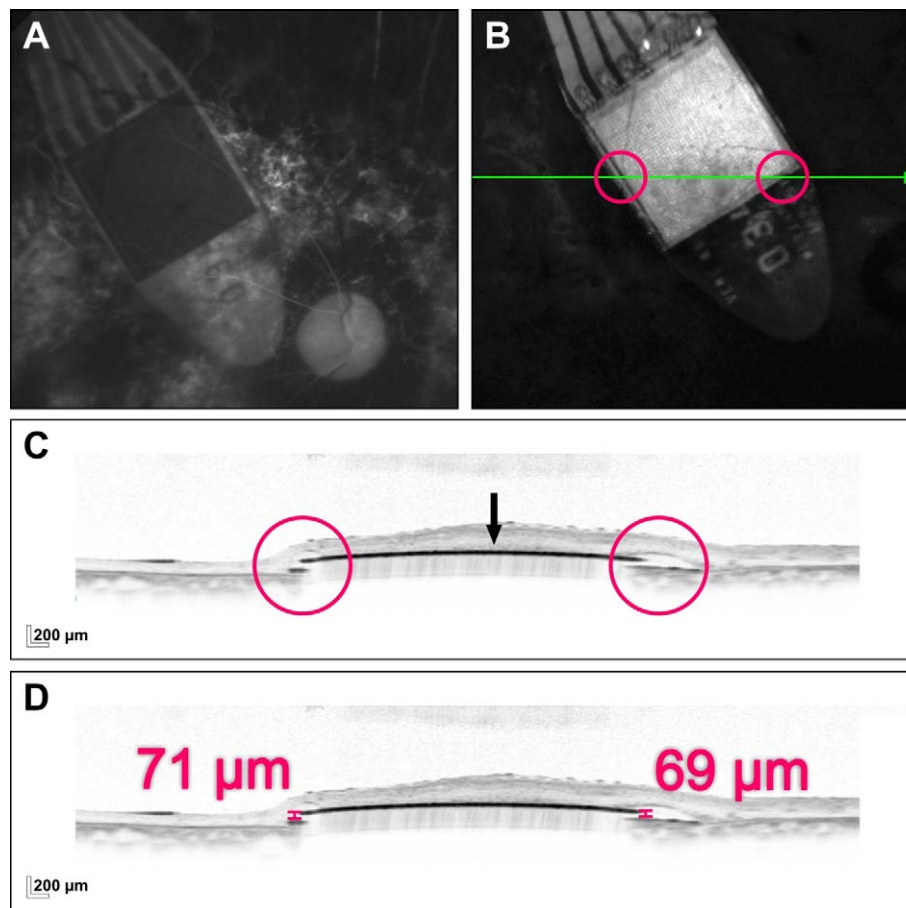


FIGURE 1. Example of subretinal implant measurement in a medium eye (subject ID: P5). (A) Red-free arterial-phase fluorescein angiography photograph of a subretinal implant with microchip on a polyamide film. (B) A cSLO image of the microchip measurement showing placement of green SD-OCT horizontal 9-mm line scan, which was captured at the retina centered on the microchip. (C) An SD-OCT image of the microchip. The *black arrow* marks the surface of the microchip. The microchip partly consists of a crystal of a silicon semiconductor; therefore, SD-OCT cannot radiate through the microchip. The *pink ring* marks the area of the edge of the microchip and the polyamide film, the carrier substrate for the microchip. (D) An SD-OCT image of the microchip thickness measurement. The example image shows the thickness measurement between the surface of the polyamide film and the surface of the microchip here in a medium eye. The thickness measurements significantly increased in SD-OCT measurements with shorter axial lengths. The flat and not tilted position of the microchip was important and was checked on the SD-OCT image before every measurement.

Subretinal Implant

The subretinal implant consists of a 70- μm thin microchip with 1500 microphotodiodes, including a sensor field area of 2800 $\mu\text{m} \times 2800 \mu\text{m}$. The carrier substrate for this microchip is a 12- μm thin polyamide film, which also carries leads for connecting the microchip to a separate power supply. Zrenner et al.⁵ showed in 2011 that a subretinal implant allows blind patients to read letters and combine them into words. A main point in maximizing the visual potential of an active subretinal implant is the proper placement of the implant⁸; therefore, careful measurements of retinal topography have to be made preoperatively to allow superior measurable outcome. The microchip is implanted under the transparent retina near the macula region. Figure 1A shows red-free arterial-phase fluorescein angiography photograph of a subretinal implant with the microchip on a polyamide film.

Heidelberg Spectralis

The SD-OCT images were taken with Heidelberg Spectralis (Heidelberg Engineering, Heidelberg, Germany). The instrument indicates measurement results on an absolute scale and

includes cSLO to monitor fundus images and SD-OCT to obtain tomographic images.

Thirty minutes after application of two drops tropicamide 0.5% (Mydratikum; Pharma Stulln, Stulln, Germany), SD-OCT scans were performed for all patients, using Heidelberg Spectralis (software version 5.3.3). All OCT scans were done by an experienced OCT operator under standardized mesopic lighting conditions. Spectral-domain OCT scans were acquired with eye tracking, and 40 frames were averaged to improve the image quality.

We chose standard SD-OCT imaging parameters currently in clinical use to capture fovea-centered line scans. We chose the same settings on all eyes in all patients. For SD-OCT (870 nm), horizontal 9-mm line scans were captured at the retina centered on the microchip.

The microchip was not tilted in the field of analyses. The flat and not tilted position of the microchip was checked on the SD-OCT image before every measurement. The microchip was scanned at different locations (15 scans per eye). Spectralis OCT camera used an internal fixation source. Nevertheless, it was very difficult to generate the SD-OCT images in patients with low stability of fixation. The operator monitored the stability of fixation with an incorporated

TABLE. The Averaged Axial Length (mm) of Each Patient and the Mean SD-OCT Thickness Measurement (μm) of 15 Images per Eye

	Subject ID							
	P1	P2	P3	P4	P5	P6	P7	P8
Axial length, mm	19.99	20.97	21.52	22.89	23.12	23.76	25.95	26.70
Mean thickness measurement, μm	84.97	84.30	79.50	72.03	70.23	69.13	64.97	63.47

infrared camera independently. Scans were repeated if image overlap was noted or if the image quality was <25 dB. If scan quality was reduced due to ocular surface dryness, they were repeated after patients were administered a drop of artificial tears.

Measuring SD-OCT thickness of the microchip of all images was performed by one trained OCT grader using the caliper tools that were part of the proprietary software (Heidelberg Eye Explorer) on the Spectralis. Figure 1B shows a cSLO image of the microchip measurement illustrating placement of a green SD-OCT horizontal 9-mm line scan that was captured at the retina centered on the microchip. Figure 1C gives an example of a thickness measurement of the microchip on an SD-OCT image. The black arrow marks the surface of the microchip. The pink ring marks the area of the edge of the microchip and the polyamide film, the carrier substrate for the microchip.

Microchips contain a silicon semiconductor crystal; therefore, SD-OCT cannot radiate through the microchip. Figure 1D shows images of the microchip thickness measurement in a medium eye.

Axial Length

We used partial coherence interferometry (version 5.02, IOL Master; Carl Zeiss Meditec, Dublin, CA, USA), a well-established tool, for measurement of the axial length of the eyes before SD-OCT thickness measurement. This noncontact method measures the distance between the corneal vertex and the retinal pigment epithelium. Ten repeated measurements of the axial length were carried out, and the average result was determined in each patient. Using IOL Master, axial length was measured in three short (<22.5 mm), three medium (22.51–25.5 mm), and two long (>25.51 mm) eyes.

Evaluation

Evaluation began by searching images where the microchip was flat and not tilted into the investigation field. Thickness measurements of the microchip were obtained by using the software calipers. Figure 1D gives an example of thickness measurements of the microchip on the SD-OCT image.

Statistical Analysis

Statistical analysis of the data was conducted using the Statistical Package for the Social Sciences software (SPSS 18.0; IBM SPSS Statistics, Chicago, IL, USA). The association between the sensor field measurements and the axial length was calculated by linear regression analysis. Quantitative variables were expressed as mean \pm standard deviation. $P < 0.05$ was considered to be statistically significant.

RESULTS

The average age of the three men and five women was 52.6 ± 16.3 years. The mean axial length was 20.8 ± 0.8 mm in short eyes, 23.3 ± 0.4 mm in medium eyes, and 26.3 ± 0.5 mm in long eyes, respectively. Emmetropia was achieved after refractive cataract surgery with posterior chamber intraocular lens (IOL) implantation. There were no intraocular factors, such as a staphyloma, for example, that could affect the results.

The SD-OCT images were taken under implant-off conditions where the visual acuity presented as stable. We measured thickness of the microchip on 15 images per eye with SD-OCT using the software calipers.

The Table shows the averaged axial length (in millimeters) of each patient and the mean microchip thickness measurement (in micrometers) using the software calipers.

We found in short eyes, in medium eyes, and in long eyes a mean value of microchip thickness measurements from SD-OCT of 82.9 ± 1.4 μm , 70.5 ± 1.3 μm , and 64.2 ± 1.3 μm , respectively.

The thickness measurements decreased in the SD-OCT measurements with longer axial lengths significantly ($P < 0.0001$). On average, the SD-OCT measurements of Heidelberg Spectralis led to correct results only in medium eyes.

Additionally, the flat and not tilted position of the microchip was of importance and was checked on the SD-OCT image before every measurement.

Figure 2 shows axial length versus mean SD-OCT microchip thickness measurement. Linear regression showed the mean thickness measurement becoming smaller as the axial length

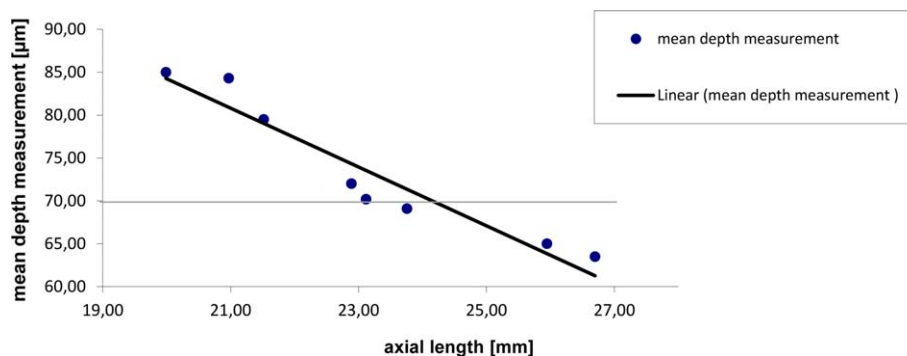


FIGURE 2. Axial length versus mean SD-OCT microchip thickness measurement. Linear regression showing that the mean thickness measurement becomes smaller as the axial length increases ($P < 0.0001$).

increased. The thickness measurements decreased with longer axial lengths significantly ($P < 0.0001$).

DISCUSSION

Our results showed accuracy of the scaling in SD-OCT thickness measurements of the Heidelberg Spectralis for emmetropic medium eyes. It is of importance for ophthalmologists to know the accuracy of the scaling of fundus imaging systems before carrying out any clinical investigation that attempts to determine absolute parameters at the fundus.^{17,18}

A century ago, Allvar Gullstrand (1862–1930) developed the first schematic model of the eye. Gullstrand's eye model is a theoretical representation that applies only to average-sized eyes.¹⁹ Measurements of a known distance, such as that of subretinal implant thickness, is a new method to prove the accuracy of these theoretical calculation models in vivo. Our results indicate the possibility of recognizing failures in theoretical formulas. As in most retinal-imaging technologies, ocular magnification characteristics of the eye must be considered for accurate analysis. Biometric factors such as corneal curvature, refractive status, anterior chamber depth, anterior segment optical power, and, in particular, the axial length, are described to be important.^{20–27} Savini et al.¹² showed influence of axial length on RNFL thickness measurements and optic disc measurements by SD-OCT. The RNFL thickness and the optic nerve head parameters decreased with longer axial lengths.¹²

Patel et al.²⁸ showed that the magnification effect of RNFL thickness measurements using SD-OCT with the Spectralis HRA+OCT can be eliminated with incorporation of transverse scaling to RNFL area measures, based on individualized ocular biometry.²⁶ Leung et al.¹¹ described that cSLO measurements of the optic disc size done with a Heidelberg Retina Tomograph (HRT 3; Heidelberg Engineering, Dossenheim, Germany) were largely independent of axial length and had a refractive error between -8 and $+4$ diopter (D).⁹ Most researchers reported that the change in OCT measurements for eyes with moderate ametropia is related linearly to axial length.^{11–16,29–31} Measures can be rescaled to match those of an emmetropic eye. Specifically, several investigators^{11,12,29} have used a modified Littmann's formula²⁰ that incorporates a magnification factor of the eye to make this correction. However, these formulas only take into account the axial length of the eye with the assumption that the interindividual variations in optics of the anterior segment have a minimal effect on the eye's principal points. We hypothesize that the direct influence of refractive error as opposed to axial length is negligible because previous studies worked out that RNFL thickness measurements do not change before and after excimer laser surgery.^{32,33} In the everyday clinical practice, SD-OCT is of decisional value for indication of treatment. Studies on diabetic macular edema³⁴ and RP³⁵ found that quantitative retinal thickness measurements can influence the therapy. However, they did not consider the axial length in central retinal thickness (CRT) measurement. More importantly, CRT is associated with visual acuity and disease severity in degenerative retinal diseases.^{36–40} The implantation of the subretinal microchip is surgically more difficult when the retina is thinner as assumed. Thus, the macular thickness provided by OCT could be a useful tool in effective selection of patients for potential use of retinal prostheses.

Nevertheless, some points should be considered before drawing hasty conclusions. The main limitation of our evaluation is the pilot nature of the observations. Studies in the future will require a larger sample size, which would increase the power of the analysis and the validity of its

findings. Other limiting factors of this evaluation are low vision status and the patients' limited ability to fixate, which also might have affected the findings.

In conclusion, axial length appears to influence the SD-OCT thickness measurements. Our results underline that caution is recommended when comparing the measured values of short and long eyes with the normative database of the instrument. Further studies with larger sample sizes are needed to confirm findings.

Acknowledgments

Disclosure: **T. Röck**, None; **K.U. Bartz-Schmidt**, None; **M. Bramkamp**, None; **D. Röck**, None

References

- Huang D, Swanson EA, Lin CP, et al. Optical coherence tomography. *Science*. 1991;254:1178–1181.
- Geitzenauer W, Hitzenberger CK, Schmidt-Erfurth UM. Retinal optical coherence tomography: past, present and future perspectives. *Br J Ophthalmol*. 2011;95:171–177.
- Horn FK, Mardin CY, Laemmer R, et al. Correlation between local glaucomatous visual field defects and loss of nerve fiber layer thickness measured with polarimetry and spectral domain OCT. *Invest Ophthalmol Vis Sci*. 2009;50:1971–1997.
- Coscas G, Coscas F, Vismara S, Souied E, Soubrane G. Spectral domain OCT in age-related macular degeneration: preliminary results with Spectralis HRA-OCT. *J Fr Ophtalmol*. 2008;31:353–361.
- Zrenner E, Bartz-Schmidt KU, Benav H, et al. Subretinal electronic chips allow blind patients to read letters and combine them to words. *Proc Biol Sci*. 2011;278:1489–1497.
- Stingl K, Greppmaier U, Wilhelm B, Zrenner E. Subretinal visual implants. *Klin Monbl Augenbeilkd*. 2010;227:940–945.
- Stingl K, Bartz-Schmidt KU, Besch D, et al. Artificial vision with wirelessly powered subretinal electronic implant alpha-IMS. *Proc Biol Sci*. 2013;280:20130077.
- Kusnyerik A, Greppmaier U, Wilke R, et al. Positioning of electronic subretinal implants in blind retinitis pigmentosa patients through multimodal assessment of retinal structures. *Invest Ophthalmol Vis Sci*. 2012;53:3748–3755.
- Stingl K, Bartz-Schmidt KU, Gekeler F, Kusnyerik A, Sachs H, Zrenner E. Functional outcome in subretinal electronic implants depends on foveal eccentricity. *Invest Ophthalmol Vis Sci*. 2013;54:7658–7665.
- Röck T, Wilhelm B, Bartz-Schmidt KU, Röck D. The influence of axial length on confocal scanning laser ophthalmoscopy and spectral-domain optical coherence tomography size measurements: a pilot study. *Graefes Arch Clin Exp Ophthalmol*. 2014;252:589–593.
- Leung CK, Cheng AC, Chong KK, et al. Optic disc measurements in myopia with optical coherence tomography and confocal scanning laser ophthalmoscopy. *Invest Ophthalmol Vis Sci*. 2007;48:3178–3183.
- Savini G, Barboni P, Parisi V, Carbonelli M. The influence of axial length on retinal nerve fibre layer thickness and optic disc size measurements by spectral-domain OCT. *Br J Ophthalmol*. 2012;96:57–61.
- Vernon SA, Rotchford AP, Negi A, Ryatt S, Tattersal C. Peripapillary retinal nerve fibre layer thickness in highly myopic Caucasians as measured by Stratus optical coherence tomography. *Br J Ophthalmol*. 2008;92:1076–1080.
- Rauscher FM, Sekhon N, Feuer WJ, Budenz DL. Myopia affects retinal nerve fiber layer measurements as determined by optical coherence tomography. *J Glaucoma*. 2009;18:501–505.

15. Budenz DL, Anderson DR, Varma R, et al. Determinants of normal retinal nerve fiber layer thickness measured by Stratus OCT. *Ophthalmology*. 2007;114:1046-1052.
16. Leung CK, Mohamed S, Leung KS, et al. Retinal nerve fiber layer measurements in myopia: an optical coherence tomography study. *Invest Ophthalmol Vis Sci*. 2006;47:5171-5176.
17. Bartz-Schmidt KU, Weber J, Heimann K. Validity of two-dimensional data obtained with the Heidelberg Retina Tomograph as verified by direct measurements in normal optic nerve heads. *Ger J Ophthalmol*. 1994;3:400-405.
18. Rudnicka AR, Burk RO, Edgar DF, Fitzke FW. Magnification characteristics of fundus imaging systems. *Ophthalmology*. 1998;105:2186-2192.
19. Rudnicka AR, Edgar DF, Bennett AG. Construction of a model eye and its applications. *Ophthalmic Physiol Opt*. 1992;12:485-490.
20. Bennett AG, Rudnicka AR, Edgar DF. Improvements on Littmann's method of determining the size of retinal features by fundus photography. *Graefes Arch Clin Exp Ophthalmol*. 1994;32:361-367.
21. Garway-Heath DF, Rudnicka AR, Lowe T, Foster PJ, Fitzke FW, Hitchings RA. Measurement of optic disc size: equivalence of methods to correct for ocular magnification. *Br J Ophthalmol*. 1998;82:643-649.
22. Sanchez-Cano A, Baraibar B, Pablo LE, Honrubia FM. Magnification characteristics of the Optical Coherence Tomograph STRATUS OCT 3000. *Ophthalmic Physiol Opt*. 2008;28:21-28.
23. Bartling H, Wanger P, Martin L. Measurement of optic disc parameters on digital fundus photographs: algorithm development and evaluation. *Acta Ophthalmol*. 2008;86:837-841.
24. Moghimi S, Hosseini H, Riddle J, et al. Measurement of optic disc size and rim area with spectral-domain OCT and scanning laser ophthalmoscopy. *Invest Ophthalmol Vis Sci*. 2012;53:4519-4530.
25. Kang SH, Hong SW, Im SK, Lee SH, Ahn MD. Effect of myopia on the thickness of the retinal nerve fiber layer measured by Cirrus HD optical coherence tomography. *Invest Ophthalmol Vis Sci*. 2010;51:4075-4083.
26. Oner V, Aykut V, Tas M, Alakus MF, Iscan Y. Effect of refractive status on peripapillary retinal nerve fibre layer thickness: a study by RTVue spectral domain optical coherence tomography. *Br J Ophthalmol*. 2013;97:75-79.
27. Littmann H. Determination of the real size of an object on the fundus of the living eye. *Klin Monbl Augenheilkd*. 1982;180:286-289.
28. Patel NB, Garcia B, Harwerth RS. Influence of anterior segment power on the scan path and RNFL thickness using SD-OCT. *Invest Ophthalmol Vis Sci*. 2012;53:5788-5798.
29. Kang SH, Hong SW, Im SK, Lee SH, Ahn MD. Effect of myopia on the thickness of the retinal nerve fiber layer measured by Cirrus HD optical coherence tomography. *Invest Ophthalmol Vis Sci*. 2010;51:4075-4083.
30. Huynh SC, Wang XY, Rochtchina E, Mitchell P. Peripapillary retinal nerve fiber layer thickness in a population of 6-year-old children: findings by optical coherence tomography. *Ophthalmology*. 2006;113:1583-1592.
31. Bendschneider D, Tornow RP, Horn FK, et al. Retinal nerve fiber layer thickness in normals measured by spectral domain OCT. *J Glaucoma*. 2010;19:475-482.
32. Dementyev DD, Kourenkov VV, Rodin AS, Fadeykina TL, Diaz Martinez TE. Retinal nerve fiber layer changes after LASIK evaluated with optical coherence tomography. *J Refract Surg*. 2005;21:623-627.
33. Sharma N, Sony P, Gupta A, Vajpayee RB. Effect of laser in situ keratomileusis and laser-assisted subepithelial keratectomy on retinal nerve fiber layer thickness. *J Cataract Refract Surg*. 2006;32:446-450.
34. Mushtaq B, Crosby NJ, Dimopoulos AT, et al. Effect of initial retinal thickness on outcome of intravitreal bevacizumab therapy for diabetic macular edema. *Clin Ophthalmol*. 2014;8:807-812.
35. Vámos R, Tátrai E, Németh J, Holder GE, DeBuc DC, Somfai GM. The structure and function of the macula in patients with advanced retinitis pigmentosa. *Invest Ophthalmol Vis Sci*. 2011;52:8425-8432.
36. Hwang YH, Kim SW, Kim YY, Na JH, Kim HK, Sohn YH. Optic nerve head, retinal nerve fiber layer, and macular thickness measurements in young patients with retinitis pigmentosa. *Curr Eye Res*. 2012;27:914-920.
37. Birch DG, Wen Y, Locke K, Hood DC. Rod sensitivity, cone sensitivity, and photoreceptor layer thickness in retinal degenerative diseases. *Invest Ophthalmol Vis Sci*. 2011;52:7141-7147.
38. Kondo M, Ito Y, Ueno S, Piao CH, Terasaki H, Miyake Y. Foveal thickness in occult macular dystrophy. *Am J Ophthalmol*. 2003;135:725-728.
39. Witkin AJ, Ko TH, Fujimoto JG, et al. Ultra-high resolution optical coherence tomography assessment of photoreceptors in retinitis pigmentosa and related diseases. *Am J Ophthalmol*. 2006;142:945-952.
40. Sandberg MA, Brockhurst RJ, Gaudio AR, Berson EL. The association between visual acuity and central retinal thickness in retinitis pigmentosa. *Invest Ophthalmol Vis Sci*. 2005;46:3349-3354.